

Decoherence in trapped ions due to polarization of the residual background gas

R. M. Serra^{1*}, N. G. de Almeida¹, W. B. da Costa², and M. H. Y. Moussa^{1†}.

¹*Departamento de Física, Universidade Federal de São*

Carlos, P. O. Box 676, São Carlos, 13565-905, São Paulo, Brazil

²*Universidade Estadual de Mato Grosso do Sul, P. O. Box 351, Dourados,*

79804-970, Mato Grosso do Sul, Brazil

We investigate the mechanism of damping and heating of trapped ions associated with the polarization of the residual background gas induced by the oscillating ions themselves. Reasoning by analogy with the physics of surface electrons in liquid helium, we demonstrate that the decay of Rabi oscillations observed in experiments on ${}^9\text{Be}^+$ can be attributed to the polarization phenomena investigated here. The measured sensitivity of the damping of Rabi oscillations with respect to the vibrational quantum number of a trapped ion is also predicted in our polarization model.

Journal-Ref: Physical Review A, **64**, 033419 (September, 2001)

PACS numbers: 32.80.Pj, 42.50.Ct, 42.50.Vk

I. INTRODUCTION

The experimental techniques developed over the last decade for manipulating trapped ions, Rydberg atoms in cavity QED, and traveling fields have enabled a fruitful dialog to take place between theoretical and experimental physics, resulting in a mastery of fundamental quantum phenomena at a level that seems to herald a new phase in the technology of communication [1] and computation [2,3]. The improvement of techniques for generating

*Electronic address: serra@df.ufscar.br

†Electronic address: miled@df.ufscar.br

and detecting nonclassical electronic and vibrational states of trapped ions and both trapped and traveling nonclassical states of the radiation field have been of growing interest in a variety of experimental applications ranging from quantum measurement concepts [4,5] to teleportation [6] and quantum logic operations [7]. In its turn, theoretical physics has exploited the possibility of engineering nonclassical states in some exotic applications such as detection of gravitational waves [8], or for measuring particular properties of the radiation field, such as its phase [9] or its Q function [10]. Laser manipulation of a string of ions in a linear trap has been proposed as a way of implementing quantum gates with cold trapped ions [2]. Furthermore, interfering laser beams have been used to induce arrays of microscopic potentials, the optical lattices [11], by the ac Stark effect, opening the way to simulated spin-spin interactions between trapped atoms, similar to those characteristic of ferromagnetism and antiferromagnetism in condensed matter physics [12]. Quantum computation with ions in thermal motion has also been suggested [13,14].

The practical realization of such interesting proposals in quantum communication and computation has come up against the decoherence of quantum states, owing to the inevitable action of the surrounding environment [15] and the intrinsic fluctuations in the interaction parameters required for logic operations [16]. In fact, the need for huge superpositions of qubit states for such operations imposes the requirements that the quantum systems be totally isolated from the environment and that the interaction parameters involved be tightly controlled. Hence, investigation of the noise sources in such promising quantum systems turns out to be a crucial step toward the implementation of a quantum logic processor.

Unlike processes in cavity QED, where decoherence is caused by the well-known cavity damping mechanisms, spontaneous atomic emission, and inefficiency of the ionization detectors, in the domain of trapped ions a large range of error sources have been identified. The effects of spontaneous emission have been studied [17–19], as well as dephasing due to the ions' zero-point motion [20]. Alternative sources of decoherence have been introduced phenomenologically [21] and stochastic models have been proposed to handle intensity and phase fluctuations in the exciting laser pulses, in addition to fluctuations in the ion trap

potential [22]. Recently, instead of a stochastic mechanism, Di Fidio and Vogel [23] have put forward a model in which the observed damping in Rabi oscillations [24] is caused by quantum jumps to an auxiliary electronic level. Other significant sources of error are the instabilities of the trap drive frequency and voltage amplitude [5,25].

Collisions of the trapped ion with residual background gas (usually H_2 in the NIST $^9\text{Be}^+$ experiments [26]) can also be an important error source, although experiments are typically carried out in a high-vacuum environment [26] at a pressure around 10^{-8} Pa. In connection with this, the current article discusses the polarization effects on the residual background gas induced by the oscillating trapped ion. We demonstrate that, apart from other known processes, the damping and heating mechanism of trapped ions is produced by local polarization of the residual thermal background gas (BG). Since the density of the BG is rather low, around 10^6 cm^{-3} [26], we do not expect to find a quasiparticle consisting of the trapped ion together with its surrounding polarization cloud, the so called polaron. The density of the BG does not permit a polaron binding energy and the trapped ion is scattered by the BG. For practical purposes, in our model we assume that the BG is continuous and that the ion is scattered by its surface oscillations, by analogy with the interaction of surface electrons in liquid helium (where the oscillations are called ripplons in their quantized form).

In contrast to loss mechanisms revealed by damped Rabi oscillations, it is well known that background gas can heat trapped ions by transferring energy during an elastic collision. A heating rate can easily be estimated from the total collision cross section [26]. Although elastic collisions are expected to be the main source of decoherence in ionic traps, inelastic collisions also take place, changing the internal state or even the species of the trapped ion. In experiments on $^9\text{Be}^+$, inelastic processes may convert the ion to BeH^+ (upon collision with a H_2 molecule) when resonant light is applied to the $^2\text{S}_{1/2} \rightarrow ^2\text{P}_{1/2,3/2}$ transitions [5]. Both types of inelastic collision, chemical reactions and charge exchange, besides depending critically on the constituents of the BG, occur only when the interparticle spacing between the trapped ion and the neutral background atoms approaches atomic dimensions. In our model, a mean interparticle spacing between the ion and the BG atoms is introduced. An

upper limit on the rate of inelastic collisions follows from the Langevin rate, which accounts for the background neutrals that penetrate the angular momentum barrier and undergo a spiraling-type collision into the ion [26,27].

The attractive interaction potential resulting from polarization of the neutral background by the electric field of the trapped ion is given by $U(r) = -\chi q^2 / (8\pi\epsilon_0 r^4)$, where χ is the polarizability and q the ionic charge. Spiraling collisions result when the impact parameter is less than a critical value $\mathbf{p} = (\chi q^2 / \pi\epsilon_0 \mathbf{m}\mathbf{v}^2)^{1/4}$, where \mathbf{m} and \mathbf{v} are the reduced mass and relative velocity of the pair. From the critical impact parameter follows the Langevin rate constant $\mathcal{L} = \pi\mathbf{p}^2\mathbf{v}$, which gives to the reaction rate $\mathcal{R} = \rho\mathcal{L} = \rho q (\pi\chi/\epsilon_0\mathbf{m})^{1/2}$, where ρ is the density of the BG. From the parameters used in the NIST ${}^9\text{Be}^+$ experiments, we obtain a small estimated probability of inelastic collisions with the BG constituents.

In addition to the chemical reactions and charge exchange, the BG can heat or cool the trapped ion through energy transfer during an elastic collision. An estimate of the elastic collision rate can be inferred from the total collision cross section σ in a Λ/r^4 potential. Assuming $\Lambda = U(r)$, it follows, from a conservative estimate, that elastic collisions will also be rare [26]. However, the effects of collisional heating (cooling), as well as the model we present here, can be tested, as suggested in Ref. [26], by raising (lowering) the BG pressure. On the other hand, it is well known that when ions are first loaded into a trap, elastic collisions with the BG are beneficial, allowing laser cooling to proceed faster, the BG providing a viscous medium and bringing the temperature of the trapped ions into thermal equilibrium with the surrounding atoms. We conclude from the work reported here that the damping medium provided by the background has also to be taken into account when the trapped ions are cooled to their motional ground state. This claim is supported by the excellent fit between our model and the experimental data for measurement of the fluorescence probability of the electronic ground state, reported in [24].

Finally, we mention that, for a linear Paul rf trap, the process of decoherence may be dominated by that of the motional state, instead of those due to internal levels, caused by a nonideal applied field [26]. In fact, the internal levels of the trapped ion are metastable, typ-

ically two ground state hyperfine sublevels [28]. While Refs. [22] take into account technical fluctuations in the applied fields used to manipulate the trapped ions, Ref. [23] attributes the error source to the coupling of the internal states to the environment. In this paper we present a model that accounts for the dominant decoherence of the ion motion in terms of the induced polarization of the BG.

The paper is organized as follows. In Sec. II we present a detailed discussion of the fundamental ion-laser and ion-BG interactions. In Sec. III we examine the effects of the ion-BG coupling on the behavior of a prepared motional-electronic state of the trapped ion, when considering the Carrier and the anti-Jaynes-Cummings ion-laser interactions. For the latter ion-laser interactions the Rabi oscillations of a trapped ion initially cooled to its motional ground state are computed under the ion-BG coupling, and our results are compared with the available experimental data for a trapped ${}^9\text{Be}^+$ ion [24]. Sec. IV is dedicated to comments and conclusions and, finally, in the Appendix A we show how to obtain a Fröhlich-type ion-BG interaction, following the model used for surface electrons in liquid helium.

II. ION-LASER AND ION-BG INTERACTIONS

We consider a single trapped ion of mass m in a one-dimensional harmonic trap of frequency ν . The ion has forbidden transitions between two internal electronic states (excited $|\uparrow\rangle$ and ground $|\downarrow\rangle$ states, assumed to be hyperfine sublevels of the ground state), separated by frequency ω_0 and indirectly coupled by the interaction with two laser beams, with frequencies ω_1 and ω_2 , in a stimulated Raman-type configuration. As indicated in Fig. 1, the laser beams are detuned by Δ from a third more excited level $|r\rangle$ which, in the stimulated Raman-type configuration, is adiabatically eliminated when Δ is much larger than three quantities: the linewidth of level $|r\rangle$, the coupling associated with the $|\uparrow\rangle \leftrightarrow |r\rangle$ and $|\downarrow\rangle \leftrightarrow |r\rangle$ transitions, and the detuning $\delta \equiv \omega_0 - \omega_L$ ($\omega_L = \omega_1 - \omega_2$) [26,28,29]. The ion interacts with an effective laser plane wave propagating along the x direction, with wave vector

$k_L = \omega_L/c$. In this configuration, only the ionic motion along the x axis will be modified. The transition between $|\downarrow\rangle$ and a fourth level $|d\rangle$, achieved by another laser strongly coupled to the electronic ground state, is analyzed in order to measure the ionic vibrational state by collecting the resonance fluorescence signal, which is the probability of the ion being found in the internal state $|\downarrow\rangle$ [30].

The ion-laser interaction Hamiltonian that describes the effective interaction of the quantized motion of the ionic center of mass (CM) coupled to its electronic degrees of freedom is [26,28,30]

$$H_{ion-laser} = \hbar\Omega \left(\sigma_+ e^{ik_L x - i\omega_L t + i\phi} + \sigma_- e^{-ik_L x + i\omega_L t - i\phi} \right), \quad (1)$$

where $\sigma_+ = |\uparrow\rangle\langle\downarrow|$, $\sigma_- = |\downarrow\rangle\langle\uparrow|$ and σ_z are the usual Pauli pseudo spin operators, x is the position operator for the x coordinate of the ion, Ω is the effective Rabi frequency of the transition $|\uparrow\rangle \leftrightarrow |\downarrow\rangle$, and ϕ is the phase difference between the two lasers.

The ion-BG interaction (the polarization of the BG induced by the oscillation of the trapped ion) will be described by a Fröhlich-type electron-phonon Hamiltonian [31]. In Appendix A we show, by analogy with surface electrons on liquid helium [32–35], that a polaron-like interaction results when the electric field of the trapped ion polarizes the neutral BG (usually H_2 in the NIST ${}^9\text{Be}^+$ experiments [26]). The attractive ion-BG interaction potential is given by $U(r) = -\chi q^2 / (8\pi\epsilon_0 r^4)$, where χ is the polarizability and q the ion charge, and the resulting Hamiltonian reads

$$H_{ion-BG} = \sum_k \hbar V_k \left(b_k e^{ikx} + b_k^\dagger e^{-ikx} \right), \quad (2)$$

where b_k^\dagger (b_k) is the creation (annihilation) operator of BG-oscillation quanta, V_k stands for the coupling strength, and k are the x -components of the BG-oscillation wave vector. In a frame rotating at the “effective laser frequency” ω_L , the ion-laser and ion-BG Hamiltonians are given in the Schrödinger picture by ($\hbar = 1$ from here on):

$$H_{ion-laser} = \Omega \left(\sigma_+ e^{i\eta_L(a+a^\dagger) - i\phi} + \sigma_- e^{-i\eta_L(a+a^\dagger) + i\phi} \right), \quad (3)$$

$$H_{ion-BG} = \sum_k V_k \left(b_k e^{i\eta_k(a+a^\dagger)} + b_k^\dagger e^{-i\eta_k(a+a^\dagger)} \right), \quad (4)$$

where $a^\dagger(a)$ is the creation (annihilation) operator of vibrational quanta, $\eta_L = k_L/\sqrt{2m\nu}$ is the Lamb-Dicke parameter, and $\eta_k = k/\sqrt{2m\nu}$ stand for Lamb-Dicke-like parameters due to the ion-BG interaction. The total Hamiltonian is given in the Schrödinger picture by $H = H_0 + H_{ion-laser} + H_{ion-BG}$, where H_0 indicates the free Hamiltonian composed of the internal and motional degrees of freedom of the trapped ion plus the BG:

$$H_0 = \nu a^\dagger a + \frac{\delta}{2} \sigma_z + \sum_k \omega_k b_k^\dagger b_k. \quad (5)$$

Writing the total Hamiltonian in the interaction picture (bold labels), by the unitary transformation $U(t) = \exp(-iH_0t)$, and then expanding the resulting expressions in terms of the parameters η_L and η_k , we get

$$\mathbf{H}_{ion-laser} = \Omega e^{-\eta_L^2/2} \left(\sum_{m,l=0}^{\infty} \frac{(i\eta_L)^{m+l}}{m!l!} \sigma_+ a^{\dagger m} a^l e^{i[(m-l)\nu+\delta]t-i\varphi} + h.c. \right), \quad (6)$$

$$\mathbf{H}_{ion-BG} = \sum_k V_k e^{-\eta_k^2/2} \left(\sum_{m,l=0}^{\infty} \frac{(i\eta_k)^{m+l}}{m!l!} b_k a^{\dagger m} a^l e^{i[(m-l)\nu-\omega_k]t} + h.c. \right), \quad (7)$$

where ion-laser resonance is achieved by tuning the laser frequencies to obtain $\delta = -\ell\nu$ ($\ell = m - l$). In what follows some reasonable approximations are made, in order to simplify considerably the Hamiltonians (6) and (7). First we mention (i) the standard Lamb-Dicke limit for the ion-laser interaction, for which $\eta_L \ll 1$ (where the ionic CM motion is strongly localized with respect to the laser wavelengths). Next, from the low energy of the BG oscillations (ii) a Lamb-Dicke-like limit, $\eta_k \ll 1$, will be assumed for the ion-BG interaction. This limit is somewhat analogous to the case of large polarons in solid state physics [36]. In fact, the motion of large polarons is continuous, as should be that of a trapped ion. In contrast, small polarons recognize the periodicity of a solid, becoming localized as in the strong coupling theory and assuming atomic dimensions. With these two approximations we obtain the simplified Hamiltonians

$$\mathbf{H}_{ion-laser} = \Omega \left(\sigma_+ e^{-i\delta t - i\varphi} + i\eta_L \sigma_+ a^\dagger e^{i(\nu+\delta)t - i\varphi} + i\eta_L \sigma_+ a e^{-i(\nu-\delta)t - i\varphi} + h.c. \right), \quad (8)$$

$$\mathbf{H}_{ion-BG} = \sum_k V_k \left(b_k e^{-i\omega_k t} + i\eta_k b_k a^\dagger e^{i(\nu-\omega_k)t} + i\eta_k b_k a e^{-i(\nu+\omega_k)t} + h.c. \right). \quad (9)$$

With the addition of (iii) the optical rotating wave approximation, three specific Hamiltonians for the ion-laser interaction are obtained, depending on the choice of the ion-laser detuning:

(a) the carrier Hamiltonian ($\delta = 0$),

$$\mathbf{H}_{ion-laser}^C = \Omega (\sigma_+ e^{-i\varphi} + \sigma_- e^{+i\varphi}), \quad (10)$$

which induces the transition $|n, \downarrow\rangle \longleftrightarrow |n, \uparrow\rangle$ (where $|n\rangle$ indicates a motional Fock state), and is responsible for rotating only the internal electronic levels of the ion wave function in accordance with

$$e^{-iH_{ion-laser}^C \tau} |n, \uparrow\rangle = \cos(\Omega\tau) |n, \uparrow\rangle - ie^{i\varphi} \sin(\Omega\tau) |n, \downarrow\rangle, \quad (11a)$$

$$e^{-iH_{ion-laser}^C \tau} |n, \downarrow\rangle = \cos(\Omega\tau) |n, \downarrow\rangle - ie^{-i\varphi} \sin(\Omega\tau) |n, \uparrow\rangle; \quad (11b)$$

(b) the Jaynes-Cummings Hamiltonian ($\delta = \nu$), corresponding to the first red sideband,

$$\mathbf{H}_{ion-laser}^{JC} = i\eta_L \Omega (\sigma_+ a e^{-i\varphi} - \sigma_- a^\dagger e^{+i\varphi}), \quad (12)$$

induces the transition $|n, \downarrow\rangle \longleftrightarrow |n-1, \uparrow\rangle$, in such a way that the electronic and vibrational modes evolve as

$$e^{-iH_{ion-laser}^{JC} \tau} |n, \uparrow\rangle = C_n |n, \uparrow\rangle - e^{-i\varphi} S_n |n+1, \downarrow\rangle, \quad (13a)$$

$$e^{-iH_{ion-laser}^{JC} \tau} |n, \downarrow\rangle = C_{n-1} |n, \downarrow\rangle + e^{i\varphi} S_{n-1} |n-1, \uparrow\rangle, \quad (13b)$$

where $C_n = \cos(g\tau\sqrt{n+1})$, $S_n = \sin(g\tau\sqrt{n+1})$, τ is the duration of the laser pulses, and $g = \eta_L \Omega$;

(c) the Anti-Jaynes-Cummings Hamiltonian ($\delta = -\nu$), corresponding to the first blue sideband,

$$\mathbf{H}_{ion-laser}^{AJC} = i\eta_L \Omega [\sigma_+ a^\dagger e^{-i\varphi} - \sigma_- a e^{+i\varphi}], \quad (14)$$

induces the transition $|n, \downarrow\rangle \longleftrightarrow |n+1, \uparrow\rangle$, and the electronic and vibrational modes evolve as

$$e^{-iH_{ion-laser}^{AJC}\tau} |n, \downarrow\rangle = C_n |n, \downarrow\rangle + e^{-i\varphi} S_n |n+1, \uparrow\rangle, \quad (15a)$$

$$e^{-iH_{ion-laser}^{AJC}\tau} |n, \uparrow\rangle = C_{n-1} |n, \uparrow\rangle - e^{i\varphi} S_{n-1} |n-1, \downarrow\rangle. \quad (15b)$$

Finally, assuming hypothesis *(iii)* and that *(iv)* the BG-oscillation modes are closely spaced in frequency, with the maximum of their spectrum far from zero, the ion-BG Hamiltonian becomes

$$\mathbf{H}_{ion-BG} = i \sum_k \eta_k V_k \left(b_k a^\dagger e^{i(\nu-\omega_k)} - b_k^\dagger a e^{-i(\nu-\omega_k)} \right), \quad (16)$$

which plays the role of a reservoir for the motional degree of freedom of the trapped ion.

Next, we analyze the effects of the ion-BG coupling on the time evolution of the ionic external and internal degrees of freedom. We note that the ion-laser detunings $\delta = \pm\nu$ cause the internal levels of the trapped ion to be affected by the BG, through the motional degree of freedom, differently from the choice $\delta = 0$, which leaves the BG without effect on the internal levels of the trapped ion.

III. EFFECTS OF THE ION-BG COUPLING ON A PREPARED MOTIONAL-ELECTRONIC STATE

In what follows, the effects of the ion-BG coupling on the behavior of a prepared motional-electronic state of the trapped ion will be considered for the ion-laser detunings $\delta = 0$ and $-\nu$, representing the Carrier and the Anti-Jaynes-Cummings ion-laser interactions discussed above.

A. Carrier Hamiltonian

First, using Glauber's P representation [37] we briefly analyze the dynamics of the ionic motional state when $\delta = 0$, the total Hamiltonian of the system, in the Schrödinger picture, being

$$\begin{aligned}
H &= H_0 + U^\dagger(t) \mathbf{H}_{ion-laser}^C U(t) + U^\dagger(t) \mathbf{H}_{ion-BG} U(t) \\
&= \nu a^\dagger a + \sum_k \omega_k b_k^\dagger b_k + \Omega (\sigma_+ e^{-i\varphi} + \sigma_- e^{+i\varphi}) + i \sum_k \eta_k V_k (b_k a^\dagger - b_k^\dagger a)
\end{aligned} \tag{17}$$

Focusing on the time evolution of the ionic motional state, which is not affected by the internal levels in the Carrier regime, we observe that the Hamiltonian (17) is analogous to that of a single-mode field trapped in a lossy cavity. The latter Hamiltonian has received considerable attention recently for computing the fidelity of a cavity-field state required for quantum communication or computation purposes [15]. In this connection, we find it interesting to analyze the decoherence process of a prepared motional state of a trapped ion due to its coupling to the BG.

Solving the coupled linear equations of motion for the operators a and b_k , we obtain from Eq. (17)

$$a(t) = u(t)a(0) + \sum_k v_k(t)b_k(0), \tag{18}$$

where, disregarding the typical small frequency shifts and introducing the damping constant Γ , the time-dependent coefficients, obeying the initial conditions $u(0) = 1$ and $v_k(0) = 0$, can be written as

$$u(t) = e^{-(\Gamma/2+i\nu)t}, \tag{19a}$$

$$v_k(t) = -\eta_k V_k e^{-i\omega_k t} \frac{1 - e^{i(\omega_k - \nu)t} e^{-\Gamma t/2}}{\Gamma/2 - i(\omega_k - \nu)}. \tag{19b}$$

From the above results, we obtain the normally ordered characteristic function $\chi_N(\xi, t)$, defined in the Schrödinger picture as the expectation value

$$\chi_N(\xi, t) = \text{Tr} \left[\rho(t) e^{\xi a^\dagger(0)} e^{\xi^* a(0)} \right], \tag{20}$$

where the density operator $\rho(t)$ refers to the composite ion-BG system, assumed, as usual, to be initially decoupled, $\rho(0) = \rho_{ion}(0)\rho_{BG}(0)$ (the ion-BG coupling is turned on suddenly at $t = 0^+$). For a motional state of the trapped ion, prepared as $\sum_l c_l |\alpha_l\rangle$, follows the representative term of the reduced density operator $\rho_{ion}(0) = |\alpha_1\rangle \langle \alpha_2|$, while for an initially thermal state with Gaussian distribution the reduced density operator for the BG reads

$$\rho_{BG}(0) = \prod_k \int \frac{e^{-|\beta_k|^2/\langle n_k \rangle}}{\pi \langle n_k \rangle} |\beta_k\rangle \langle \beta_k| d^2\beta_k. \quad (21)$$

From the characteristic function (20) we derive the conditional distribution function

$$\begin{aligned} P(\gamma, t) &= \frac{1}{\pi^2} \int e^{\gamma\xi^* - \gamma^*\xi} \chi_N(\xi, t) d^2\xi \\ &= \frac{\langle \alpha_1 | \alpha_2 \rangle}{\pi D(t)} \exp \left[-\frac{(\gamma^* - u^*(t)\alpha_1^*)(\gamma - u(t)\alpha_2)}{D(t)} \right], \end{aligned} \quad (22)$$

whose dispersion is given by $D(t) = \sum_k \langle n_k \rangle |v_k(t)|^2 = \bar{n}_{th} (1 - e^{-\Gamma t})$, where the occupation number of the BG-oscillations in thermal equilibrium reads $\bar{n}_{th} = (e^{-\nu/k_B T} - 1)^{-1}$, k_B is the Boltzmann constant, and T is the absolute temperature. Fig. 2 display the damping process in the evolution of the conditional distribution function $P(\gamma, t)$ for a prepared motional coherent state. The rotation in phase space arises from the factor $\exp(-i\nu t)$ in Eq. (19a) and we observe both the effects coming from the environment: the loss of excitation, carrying the initial coherent state to the vacuum state, and the diffusion due to the nonzero temperature of the BG. These effects are clearly seen from the shape of the distribution function $P(\gamma, t)$ depicted in Fig. 2 at $\Gamma t = 0.2$ and 0.9 .

From the distribution function $P(\gamma, t)$, we can obtain the reduced density operator for the ion,

$$\rho_{ion}(t) = \frac{1}{\pi^2} \int P(\gamma, t) |\gamma\rangle \langle \gamma| d^2\gamma, \quad (23)$$

and the mean value of operators associated with the ionic motional states; for example, the mean excitation of a prepared motional vacuum state, i.e., $\alpha_1 = \alpha_2 = 0$, reads

$$\langle a^\dagger(t)a(t) \rangle = \int P(\alpha, t) \alpha^* \alpha d^2\alpha = D(t), \quad (24)$$

showing the heating process of the motional vacuum state due to a thermal BG.

B. Anti-Jaynes-Cummings Hamiltonian

Next, we examine the action of the ion-BG coupling on a prepared motional-electronic state of the trapped ion when $\delta = -\nu$, the total Hamiltonian being

$$\begin{aligned}
H &= H_0 + U^\dagger(t) \mathbf{H}_{ion-laser}^{AJC} U(t) + U^\dagger(t) \mathbf{H}_{ion-BG} U(t) \\
&= \nu a^\dagger a - \frac{\nu}{2} \sigma_z + \sum_k \omega_k b_k^\dagger b_k + i\eta_L \Omega (\sigma_+ a^\dagger e^{-i\varphi} - \sigma_- a e^{+i\varphi}) + i \sum_k \eta_k V_k (b_k a^\dagger - b_k^\dagger a). \quad (25)
\end{aligned}$$

We are considering the Anti-Jaynes-Cummings (instead of the Jaynes-Cummings) Hamiltonian for the ion-laser interaction, so as to compute, in this regime, the damping of the Rabi oscillations of a trapped ion initially cooled to its motional ground state and to compare our results with the available experimental data for a trapped ${}^9\text{Be}^+$ ion [24].

To compute the atomic inversion from Hamiltonian (25), we use the techniques developed to investigate the Jaynes-Cummings Hamiltonian for an atom interacting with a monochromatic field trapped in a lossy cavity at a finite temperature, which is analogous to Eq. (25) and has received considerable attention in the literature [38–41]. The standard master-equation technique was employed in Ref. [39] to obtain the density matrix for the combined atom-field system in the interaction picture. However, following [38], we calculate the evolution of the atomic inversion from the time-dependent averages of atomic excitation, photon numbers, and other field quantities. Although also based on the master-equation approach, the technique in [38] consists of working with a hierarchy of c -number quantities derived from the equation of motion for any operator of the form $(a^\dagger)^m a^n \mathcal{O}_A$ (where \mathcal{O}_A is an atomic operator), given by

$$\begin{aligned}
\frac{d}{dt} [(a^\dagger)^m a^n \mathcal{O}_A] &= -i \left[(a^\dagger)^m a^n \mathcal{O}_A, -\frac{\nu}{2} \sigma_z + i\eta_L \Omega (\sigma_+ a^\dagger e^{-i\varphi} - \sigma_- a e^{+i\varphi}) \right] \\
&\quad + \left\langle \frac{d}{dt} [(a^\dagger)^m a^n] \right\rangle_{BG} \mathcal{O}_A, \quad (26)
\end{aligned}$$

where the last term includes the commutation relation between $(a^\dagger)^m a^n \mathcal{O}_A$ and the components of the Hamiltonian (25) describing the energy of the BG and its interaction with the ionic external modes, as well as the motional energy of the trapped ion. Under the Wigner-Weisskopf (WW) approximation and supposing that the BG is in thermal equilibrium, we obtain [41]

$$\begin{aligned}
\left\langle \frac{d}{dt} [(a^\dagger)^m a^n] \right\rangle_{BG} &= \left(i\nu(m-n) - \frac{\Gamma}{2}(m+n) \right) \langle (a^\dagger)^m a^n \rangle_{BG} \\
&\quad + \Gamma m n \bar{n}_{th} \langle (a^\dagger)^{m-1} a^{n-1} \rangle_{BG}. \quad (27)
\end{aligned}$$

The damping constant, arising from the WW approximation, is $\Gamma = 2\pi [g(\nu)]^2 \Lambda(\nu)$, where $g(\nu) \equiv g_{\nu/c}$ is the coupling constant evaluated at $k = \nu/c$ and $\Lambda(\nu) = \mathbb{V}\nu^2/\pi c^3$ (\mathbb{V} being the quantization volume) is the density of states. The occupation number \bar{n}_{th} follows from the assumption of thermal equilibrium, where the noise operators $\mathcal{N}(t) = \sum_k g_k b_k(0) e^{-i(\omega_k - \nu)t}$ (with $g_k = \eta_k V_k$) satisfy $\langle \mathcal{N}(t) \rangle_{BG} = \langle \mathcal{N}^\dagger(t) \rangle_{BG} = 0$, and $\langle \mathcal{N}^\dagger(t) \mathcal{N}(t') \rangle_{BG} = \Gamma \bar{n}_{th} \delta(t - t')$ (see Ref. [41]).

From Eqs. (26) and (27) we derive the time-evolution of the atomic inversion $\langle \sigma_z \rangle$ and the motional occupation number of the trapped ion $\langle a^\dagger a \rangle$:

$$\frac{d\langle \sigma_z \rangle}{dt} = 2g \langle \sigma_+ a^\dagger e^{-i\varphi} + \sigma_- a e^{+i\varphi} \rangle, \quad (28)$$

$$\frac{d\langle a^\dagger a \rangle}{dt} = g \langle \sigma_+ a^\dagger e^{-i\varphi} + \sigma_- a e^{+i\varphi} \rangle - \Gamma \langle a^\dagger a \rangle + \Gamma \bar{n}_{th} \quad (29)$$

with the angular brackets denoting the BG as well as the quantum mechanical average. Eqs. (28) and (29) involve the average of the Hermitian operator $\sigma_+ a^\dagger e^{-i\varphi} + \sigma_- a e^{+i\varphi}$ whose equation of motion involves the quantity $\langle a^\dagger a \sigma_z \rangle$. In its turn, the equation of motion of this quantity involves higher-order products of averaged operators such as $\langle (a^\dagger)^2 a^2 \rangle$, $\langle (a^\dagger)^2 a^2 \sigma_z \rangle$, and so on. To deal with such averaged operators it is convenient to define the c -numbers variables

$$\mathcal{P}_n = \langle (a^\dagger)^n a^n \rangle, \quad n \geq 0, \quad \mathcal{P}_0 = 1; \quad (30a)$$

$$\mathcal{Q}_n = \langle (a^\dagger)^n a^n \sigma_z \rangle, \quad n \geq 0, \quad \mathcal{Q}_0 = \langle \sigma_z \rangle; \quad (30b)$$

$$\mathcal{R}_n = \langle \sigma_+ (a^\dagger)^n a^{n-1} e^{-i\varphi} + \sigma_- (a^\dagger)^{n-1} a^n e^{+i\varphi} \rangle, \quad n > 0. \quad (30c)$$

Solving the dynamical equations for the above c -number variables we obtain the dynamics of the atomic inversion and the motional occupation number of the trapped ion. From definitions (30a)-(30c), and Eqs. (26) and (27) we obtain the following set of equations

$$\frac{d\mathcal{P}_n}{dt} = ng\mathcal{R}_n - n\Gamma\mathcal{P}_n + n^2\Gamma\bar{n}_{th}\mathcal{P}_{n-1}, \quad (31a)$$

$$\frac{d\mathcal{Q}_n}{dt} = ng\mathcal{R}_n + 2g\mathcal{R}_{n+1} - n\Gamma\mathcal{Q}_n + n^2\Gamma\bar{n}_{th}\mathcal{Q}_{n-1}, \quad (31b)$$

$$\frac{d\mathcal{R}_n}{dt} = -2g\mathcal{Q}_n + ng\mathcal{P}_{n-1} - ng\mathcal{Q}_{n-1} - (n-1/2)\Gamma\mathcal{R}_n + n(n-1)\Gamma\bar{n}_{th}\mathcal{R}_{n-1}. \quad (31c)$$

Note that at zero temperature ($\bar{n}_{th} = 0$) and an initially prepared ionic state $|n = 0, \downarrow\rangle$ we obtain a closed set of equations, since the expectation value of the operators involving quadratic or higher powers of the ionic motional operators a and a^\dagger are therefore zero at all times [41]. However, to compare the decay of Rabi oscillations resulting from our model with the experimental data [24], we have to deal with the realistic case of non-zero temperature. Observing that for the initially prepared ionic state $|n = 0, \downarrow\rangle$, the Anti-Jaynes-Cummings Hamiltonian induces the transition $|0, \downarrow\rangle \longleftrightarrow |1, \uparrow\rangle$, and it is possible to estimate a temperature around ν/k_B for the trapped ion and, consequently, for the BG. In fact, under such conditions the thermal energy of the trapped ion $k_B T$ is around ν , resulting in a motional occupation number around unity ($\bar{n}_{th} \approx 1$). On the other hand, since the Rabi oscillations in NIST experiments [24] survive considerably above $100\mu s$, it is possible to estimate a damping factor Γ around $10^{-3}s$. Having these values at hand and truncating the system of equations (31a)-(31c) at $n = 4$ (an approximation due to the low motional occupation number estimated above for the BG), we obtain, via the numerical Laplace transform method, the time-evolution of the probability for fluorescence measurement of the electronic ground state $P_\downarrow(t) = (1 - \langle\sigma_z\rangle)/2$. Fig. 3 displays the behavior of the function $P_\downarrow(t)$ computed from our model, which is in excellent agreement with the experimental data reported in [24]. We used in our numerical calculation the experimental parameters $\eta_L = 0.202$ and $\Omega/2\pi \approx 475$ kHz. In particular, our model reproduces the asymmetry of the decay of Rabi oscillations seen in the experimental data. To obtain such behavior, we used the parameters $\bar{n}_{th} = 1.0$ and $\Gamma/g = 6.0 \times 10^{-3}$, which are in good agreement with the values estimated above. It is worth noting that, when switching off the laser pulse, Eq. (24) indicates that the motional occupation number of the trapped ion $\langle a^\dagger a \rangle$ goes asymptotically to unity, as expected.

In order to demonstrate from our model the sensitivity of the damping of Rabi oscillations to the motional quantum number, we depicted in Figs. 4(a,b) the behavior of the function $P_\downarrow(t)$ computed from our model (full lines) when the initially prepared ionic states are $|n = 0, \downarrow\rangle$ [Fig. 4(a)] and $|n = 1, \downarrow\rangle$ [Fig. 4(b)]. Figs. 4(a,b) also display the heuristic

relation used in [24] for fitting the experimental data,

$$P_{\downarrow}(t) \approx \frac{1}{2} \left(1 + \sum_n p_n \cos(2\Omega t \sqrt{n+1}) e^{-\gamma_n t} \right), \quad (32)$$

where p_n is the initial probability distribution of the motional states in the Fock basis and $\gamma_n = \gamma_0(n+1)^{0.7}$ is a phenomenological damping rate. The behavior of the heuristic relation (32) for $|n=0, \downarrow\rangle$ (Fig. 4(a)) and $|n=1, \downarrow\rangle$ (Fig. 4(b)) is shown in dotted lines using the value $\gamma_0 = 11.9(4)$ kHz estimated in [24]. We stress that Eq. (32) describes a symmetric decay of the Rabi oscillations instead of the experimentally observed asymmetry which is in agreement with our model (see Fig. 3). Therefore, we claim that the polarization of the residual background gas is the mechanism leading to the n -dependence of the decoherence effects of a trapped ion.

IV. COMMENTS AND CONCLUSIONS

We have proposed an alternative mechanism to explain the damping of Rabi oscillations of a ${}^9\text{Be}^+$ ion initially cooled to its motional ground state. Our model allows for the influence of the polarization of the residual background gas induced by the oscillating trapped ion. The polarization of the BG, which in turn influences the trapped ion motion, is described by a Fröhlich-type ion-BG interaction with a Lamb-Dicke-like limit where $\eta_k = k/\sqrt{2m\nu} \ll 1$, k being the BG oscillation wave vectors, and m (ν) being the mass (frequency) of the trapped ion.

Since experiments on trapped ions are carried out in a high-vacuum environment, the density of the BG, around 10^6 cm^{-3} [26], does not permit a polaron binding energy and the trapped ion is scattered by the BG. Both elastic and inelastic collisions are present, although elastic collisions are expected to be the main source of decoherence. The troublesome inelastic processes of chemical reactions and charge exchange are expected to be rare. Although a conservative estimate for the elastic collisions rate also leads to a small value, we claim that the damping medium provided by the background, which allows laser-cooling

to proceed faster when ions are first loaded into a trap, has also to be taken into account when the trapped ions are cooled to their motional ground state. As mentioned in [26], for a linear Paul-rf trap the main source of decoherence may be associated with errors arising from the external degrees of freedom of the trapped ion rather than internal levels or a nonideal applied field.

Under the Lamb-Dicke-like limit adopted here, the resulting ion-BG interaction consisting of the standard “rotating wave” terms (assuming that the spectrum of the phonon modes presents its maximum far from zero) turns out to be the usual linear response model of the reservoir (the BG) to the system (the trapped ion) [37,42]. Glauber’s P representation was used to analyze the dynamics of the ionic motional state when considering a Carrier pulse for the ion-laser interaction. The Carrier pulse prevents the BG having any effect on the internal levels of the trapped ion and either the damping or the heating process of the ionic motional state, depending on the temperature of the BG, was investigated. On the other hand, a master-equation approach was used to achieve a theoretical fit to the exponentially decaying, sinusoidal Rabi oscillations [24] resulting from a prepared motional-electronic state of the trapped ion under the anti-Jaynes-Cummings pulse.

The complete agreement between the measured data for Rabi oscillations with the behavior computed from our model indicates that polarization effects constitute a relevant source of error in the ionic trap. Evidently, the error from polarization of the BG has to be taken together with the errors coming from the internal levels and the application of a nonideal field [26], as investigated in Refs. [22,23]. Like the stochastic approach in [23], our model also reproduces the asymmetry of the decay of Rabi oscillations, as observed in the experimental data. Since the authors in Ref. [23] claim that the asymmetry of the measured data is consistent with the assumption of the mechanism of quantum jumps, we mention that it is also consistent with the damping-heating competition produced by the ion-BG interaction (through the motional occupation number \bar{n}_{th} and the damping factor Γ). Moreover, the consistency of our model is confirmed by the fact that the best fit of the measured data was accomplished with parameter values ($\bar{n}_{th} = 1.0$ and $\Gamma/g = 6.0 \times 10^{-3}$) in

agreement with theoretical estimates.

Finally, we have demonstrated with our model that the damping of Rabi oscillations is sensitive to the motional quantum number, as experimentally observed. The behaviour of the curves in Figs. 4(a,b), representing two ionic states initially prepared with different motional quantum numbers $|n = 0, \downarrow\rangle$ and $|n = 1, \downarrow\rangle$, respectively, strongly suggests that the polarization of the residual background gas is the mechanism leading to the n -dependence of the decoherence effects of a trapped ion.

Acknowledgments

We wish to express thanks for the support from CNPq and FAPESP, Brazilian agencies. We also thank S. S. Sokolov and N. Studart for helpful discussions and D. J. Wineland and C. Monroe for sending us the experimental data used in Fig. 3.

Appendix A

In this appendix, reasoning by analogy with the physics of surface electrons on liquid helium [34,35], we show how to obtain a Fröhlich-type ion-BG interaction. For practical reason, we assume a continuous BG and a cylindrical symmetry for the ion-BG system, as depicted in Fig. 5. The ion, oscillating along the x -axis, is assumed to be at a distance z from the origin of the coordinate system which is fixed in the center of the BG surface located in the xy -plane. This distance z (which contributes to the coupling parameter V_k) is here assumed to be a mean distance between the ion and the atoms composing the BG, a mean interparticle spacing between two colliding partners. As mentioned in the Introduction, the ion is scattered by the oscillations of the BG surface, whose dynamic roughness is given by $\xi(\vec{r}^I)$ (see Fig. 5).

The potential energy of the ion due to polarization of the BG is

$$\mathcal{U}(\vec{r}, z) = -\frac{\chi q^2}{2} \int d^2 \vec{r}^I \int_{-\infty}^{\xi(\vec{r}^I)} dz' \frac{1}{\left[\left| \vec{r}^I - \vec{r} \right|^2 + (z' - z)^2 \right]^2}.$$

Substituting the variables $z - \xi(\vec{r}') = \zeta$, $z' - \xi(\vec{r}') = \zeta'$, and defining $\Lambda/\pi \equiv \chi\rho e^2/2$, we can rewrite the potential energy as

$$\begin{aligned}\mathcal{U}(\vec{r}, z) &= \delta\mathcal{U}(\vec{r}, z) + \mathcal{U}_0(\vec{r}, z), \\ \delta\mathcal{U}(\vec{r}, z) &= -\frac{\Lambda}{\pi} \int d^2\vec{r}' \int_0^\xi(\vec{r}') - \xi(\vec{r}) d\zeta' \frac{1}{\left[|\vec{r}' - \vec{r}|^2 + (\zeta' - \zeta)^2\right]^2}, \\ \mathcal{U}_0(\vec{r}, z) &= -\frac{\Lambda}{\pi} \int d^2\vec{r}' \int_\infty^0 d\zeta' \frac{1}{\left[|\vec{r}' - \vec{r}|^2 + (\zeta' - \zeta)^2\right]^2}.\end{aligned}$$

Assuming that the roughness of the BG, $\xi(\vec{r}') - \xi(\vec{r})$, is sufficiently small and expanding $\xi(\vec{r}')$ and $\xi(\vec{r})$ in Fourier series we obtain

$$\begin{aligned}\delta\mathcal{U}(\vec{r}, z) &\approx -\frac{\Lambda}{\pi} \int d^2\vec{r}' \left. \frac{\xi(\vec{r}') - \xi(\vec{r})}{\left[|\vec{r}' - \vec{r}|^2 + (z' - z)^2\right]^2} \right|_{z'=0} \\ &= \frac{\Lambda}{\pi\sqrt{S}} \sum_{\vec{k}} \xi(\vec{k}) e^{i\vec{k}\cdot\vec{r}} \left[\int \frac{d^2\vec{\lambda}}{(\lambda^2 + z^2)^2} - \int \frac{d^2\vec{\lambda} e^{i\vec{k}\cdot\vec{\lambda}}}{(\lambda^2 + z^2)^2} \right],\end{aligned}$$

where S is the area of the BG surface and we have substituted the variable $\vec{r}' - \vec{r} = \vec{\lambda}$. After integrating over $\vec{\lambda}$ we obtain the perturbed potential energy

$$\delta\mathcal{U}(\vec{r}, z) \approx \sum_{\vec{k}} \xi(\vec{k}) e^{i\vec{k}\cdot\vec{r}} \frac{\Lambda}{z\sqrt{S}} \left[\frac{1}{z} - kK_1(kz) \right],$$

where $K_1(kz)$ is the modified Bessel function. At this point we can quantize the dynamic variable $\xi(\vec{k})$ as follows [34]:

$$\begin{aligned}\xi(\vec{k}) &= C_{\vec{k}} \left(a_{\vec{k}} + a_{-\vec{k}}^\dagger \right), \\ C_{\vec{k}} &= \sqrt{\frac{\hbar}{2\rho\omega(\vec{k})}}\end{aligned}$$

where $\omega(\vec{k})$ is the dispersion relation. Defining the coupling parameter

$$V_{\vec{k}} = \frac{\Lambda C_{\vec{k}}}{z\sqrt{S}} \left[\frac{1}{z} - kK_1(kz) \right],$$

we finally obtain the ionic quantized potential energy due to interaction with the BG as

$$\mathcal{U}(\vec{r}, z) = \sum_{\vec{k}} V_{\vec{k}} \left(a_{\vec{k}} + a_{-\vec{k}}^\dagger \right) e^{i\vec{k} \cdot \vec{r}} + \mathcal{U}_0(\vec{r}, z),$$

which results, in one dimension, in the interaction Hamiltonian (2). $\mathcal{U}_0(\vec{r}, z)$ plays the role of a reference energy.

- [1] J. I. Cirac, P. Zoller, H. J. Kimble, and H. Mabuchi, Phys. Rev. Lett. **78**, 3221 (1997); T. Pellizzari, Phys. Rev. Lett. **79**, 5242 (1997).
- [2] J. I. Cirac and P. Zoller, Phys. Rev. Lett. **74**, 4091 (1995).
- [3] Q. A. Turchette, C. J. Hood, W. Lange, H. Mabuchi, and H. J. Kimble, Phys. Rev. Lett. **75**, 4710 (1995); I. L. Chuang, L. M. K. Vandersypen, X. Zhou, D. W. Leung, and S. Lloyd, *Nature*, **393**, 143 (1998); B. E. Kane, *Nature* **393**, 143 (1998).
- [4] M. Brune, E. Hagley, J. Dreyer, X. Maitre, A. Maali, C. Wunderlich, J. M. Raimond, and S. Haroche, Phys. Rev. Lett. **77**, 4887 (1996).
- [5] C. Monroe, D. M. Meekhof, B. E. King, and D. J. Wineland, *Science* **272**, 1131 (1996).
- [6] A. Furasawa, J. L. Sorensen, S. L. Braunstein, C. A. Fuchs, H. J. Kimble, and E. S. Polzik, *Science* **282**, 706 (1998); S. L. Braunstein, and H. J. Kimble, Phys. Rev. Lett. **80**, 869 (1998).
- [7] C. Monroe, D. M. Meekhof, B. E. King, W. M. Itano, and D. J. Wineland, Phys. Rev. Lett. **75**, 4714 (1995).
- [8] J. N. Hollenhorst, Phys. Rev. D **19**, 1669 (1979).
- [9] S. M. Barnett and D. T. Pegg, Phys. Rev. Lett. **76**, 4148 (1996).
- [10] B. Baseia, M. H. Y. Moussa, and V. S. Bagnato, Phys. Lett. A **231**, 331 (1997).

- [11] D. Jaksch, C. Bruder, J. I. Cirac, C. W. Gardiner, and P. Zoller, Phys. Rev. Lett. **81**, 3108 (1998).
- [12] A. Sorensen and K. Molmer, Phys. Rev. Lett. **83**, 2274 (1999).
- [13] J. F. Poyatos, J. I. Cirac, and P. Zoller, Phys. Rev. Lett. **81**, 1322 (1998).
- [14] A. Sorensen and K. Molmer, Phys. Rev. A **62**, 022311 (2000).
- [15] N. G. de Almeida, R. Napolitano, and M. H. Y. Moussa, Phys. Rev. A **62**, 033815 (2000);
N. G. de Almeida, P.B. Ramos, R. M. Serra, and M. H. Y. Moussa, J. Opt. B: Quantum Semiclass. Opt. **2**, 792 (2000).
- [16] R. M. Serra, P. B. Ramos, N. G. de Almeida, W. D. José, and M. H. Y. Moussa, Phys. Rev. A. **63**, 053813 (2001)
- [17] R. J. Hughes, D. F. V. James, E. H. Knill, R. Laflamme, and A. G. Petschek, Phys. Rev. Lett. **77**, 3240 (1996).
- [18] M. B. Plenio and P. L. Knight, Proc. R. Soc. London A **453**, 2017 (1997).
- [19] D. F. V. James et al., in *Photonic Quantum Computing, Proceedings of SPIE 3076*, edited by S. P. Hotaling and A. R. Pirich (SPIE, Bellingham, 1997), pp. 42-50. See also D. F. James, Phys. Rev. Lett. **81**, 3417 (1998).
- [20] A. Garg, Phys. Rev. Lett. **77**, 964 (1996).
- [21] M. Muraio and P. L. Knight, Phys. Rev. A **58**, 663 (1998).
- [22] S. Schneider and G. J. Milburn, Phys. Rev. A **57**, 3748 (1998); S. Schneider and G. J. Milburn, Phys. Rev. A **59**, 3766 (1999).
- [23] C. Di Fidio and W. Vogel, Phys. Rev. A **62**, 031802(R) (2000).
- [24] D. M. Meekhof, C. Monroe, B. E. King, W. M. Itano, and D. J. Wineland, Phys. Rev. Lett. **76**, 1796 (1996); **76**, 2346(E) (1996).

- [25] C. Roos , Th. Zeiger, H. Rohde, H. C. Nägerl , J. Eschner, D. Leibfried, F. Schmidt-Kaler, and R. Blatt, Phys. Rev. Lett. **83**, 4713 (1999).
- [26] D. J. Wineland, C. Monroe, W. M. Itano, D. Leibfried, B. E. King, and D. M. Meekhof, J. Res. Natl. Inst. Stand. Technol. **103**, 259 (1998).
- [27] J. B. Hasted, *Physics of Atomic Collisions*, (Butterworth & Co., New York, 1972).
- [28] L. Davidovich, M. Orszag, and N. Zagury, Phys. Rev. A **54**, 5118 (1996).
- [29] J. Steinbach, J. Twamley, and P. L. Knight, Phys. Rev. A **56**, 4815 (1997); H. Zeng, Y. Wang and Y. Segawa, Phys. Rev. A **59**, 2174 (1999).
- [30] D. Leibfried, D. M. Meekhof, B. E. King, C. Monroe, W. M. Itano, and D. J. Wineland, Phys. Rev. Lett. **77**, 4281 (1996);
W. M. Itano ,C. Monroe, D. M. Meekhof, D. Leibfried, B. E. King, and D. J. Wineland, quan-ph/9702038 (1997);
D. Leibfried, D. M. Meekhof, C. Monroe, B. E. King W. M. Itano, and D. J. Wineland, J. Mod. Opt. **44**, 2485 (1997); D. M. Meekhof, D. Leibfried, C. Monroe, B. E. King W. M. Itano, and D. J. Wineland, Brazilian. J. Phys. **27**, 178 (1997).
- [31] H. Fröhlich, in: *Polarons and Excitons*, edited by C. Kuper and G. Whitfield (Oliver and Boyd, Edinburgh, 1963).
- [32] E. M. Lifshitz, Zh. Eksp. Teor. Fiz. **29**, 94 (1956) [Sov. Phys. JETP **2**, 73 (1956)].
- [33] E. S. Sabisky and C. H. Anderson, Phys. Rev. A **7**, 790 (1973).
- [34] V. B. Shikin and Yu P. Monarka, J. Low Temp. Phys. **16**, 193 (1974).
- [35] N. Studart and S. S. Sokolov, in *Two-Dimensional Electron System*, edited by E. Y. Andrei (Kluwer Academic Publishers, Dordrecht, 1997).
- [36] F. M. Peeters and J. T. Devreese, Phys. Rev. B **23**, 1936 (1981).

- [37] B. R. Mollow and R. J. Glauber, Phys. Rev. **160**, 1076 (1967); *ibid.* **160**, 1097 (1967).
- [38] S. Sachdev, Phys. Rev. A **29**, 2627 (1984).
- [39] S. M. Barnett, Ph.D. thesis, University of London, 1985; S. M. Barnett and P. L. Knight, Phys. Rev. A **33**, 2444 (1986).
- [40] N. Nayak, R. K. Bullough, B. V. Thompson, and G. S. Agarwal, IEEE J. Quantum Electron. **24**, 1331 (1988).
- [41] M. O. Scully and S. Zubairy, *Quantum Optics* (Cambridge University Press, Cambridge, England, 1997).
- [42] A.O. Caldeira and A.J. Leggett, Ann. Phys. (N.Y.) **149**, 374 (1983); **153**, 445(E) (1984); A.O. Caldeira and A.J. Leggett, Physica A **121**, 587 (1983); **130**, 374(E) (1985).

Figure Captions

FIG. 1. Electronic energy level diagram of a trapped ion interacting with laser beams of frequency ω_1 and ω_2 , where $\delta = \omega_0 - \omega_1 + \omega_2$ ($\delta \ll \Delta$), $|r\rangle$ (adiabatically eliminated) is an auxiliary electronic level which indirectly couples the levels $|\uparrow\rangle$ and $|\downarrow\rangle$, and $|d\rangle$ is an electronic level used to measure the fluorescence emission.

FIG. 2. Conditional distribution function $P(\gamma, t)$ for an initially prepared motional coherent state depicted at $\Gamma t = 0.2$ and 0.9 . The mean value of the amplitude moves on an exponential spiral displaying both the effects due to coupling with the environment: the loss of excitation, which carries the initial coherent state to the vacuum state, and the diffusion due to nonzero temperature of the BG.

FIG. 3. Time evolution of the probability of fluorescence measurement of the electronic ground state $P_{\downarrow}(t)$, computed from our model (full line) and measured in the NIST ${}^9\text{Be}^+$ experiments [24] (dots). The parameters used in the experiments $\eta_L = 0.202$ and $\Omega/2\pi \approx 475$ kHz, were adopted for the numerical calculation, together with the values $\bar{n}_{th} = 1.0$ and $\Gamma/g = 6.0 \times 10^{-3}$ which are in good agreement with theoretical estimates.

FIG. 4. Time evolution of the probability of fluorescence measurement of the electronic

ground state $P_{\downarrow}(t)$ for the initially prepared ionic states (a) $|n = 0, \downarrow\rangle$ and (b) $|n = 1, \downarrow\rangle$, according to our model (full lines) and the heuristic relation (32) (dotted lines), demonstrating the measured sensitivity of the damping of Rabi oscillations to the motional quantum number [24].

FIG. 5. Sketch of ion-BG interaction, showing the ion oscillating in the x -direction, assumed to be at a distance z from the origin of the coordinate system which is fixed in the center of the BG surface located in the xy -plane. The ion is scattered by the oscillations of the BG surface, whose dynamic roughness is given by $\xi(\vec{r}')$.

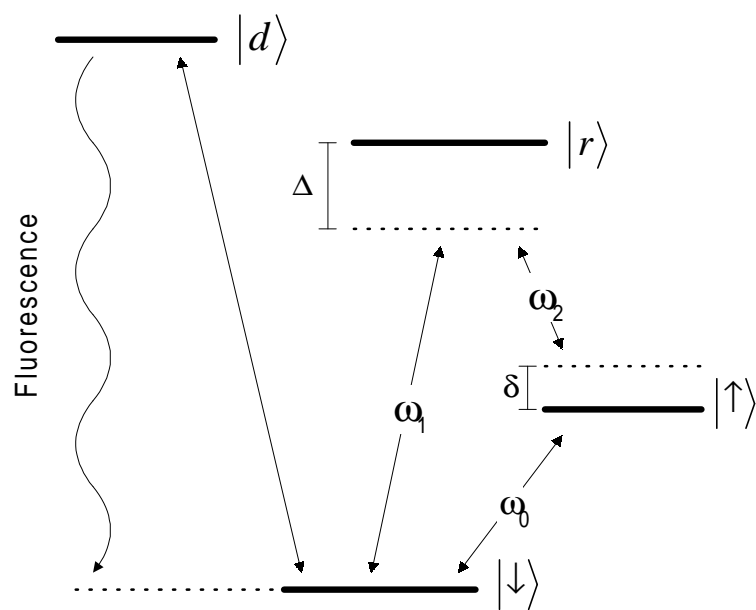


Fig. 1

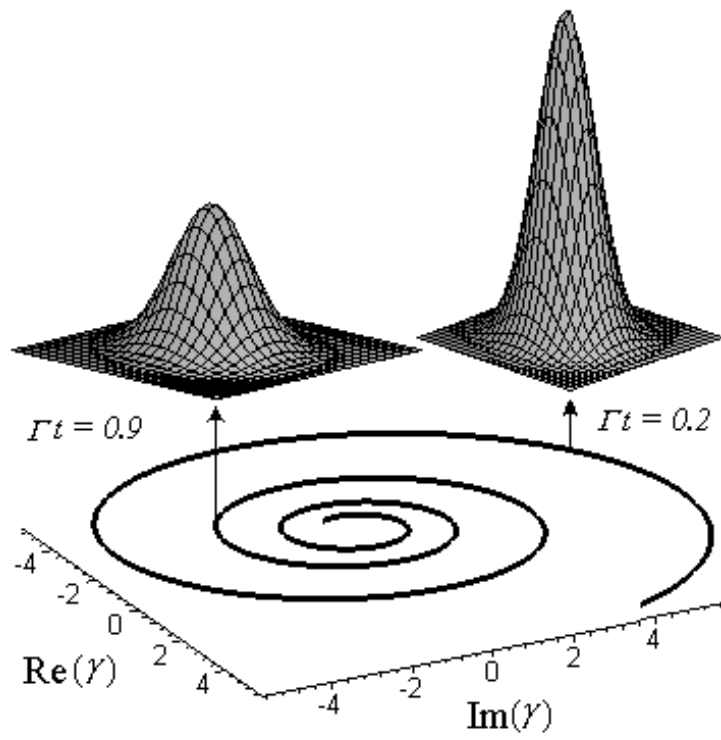


FIG. 2

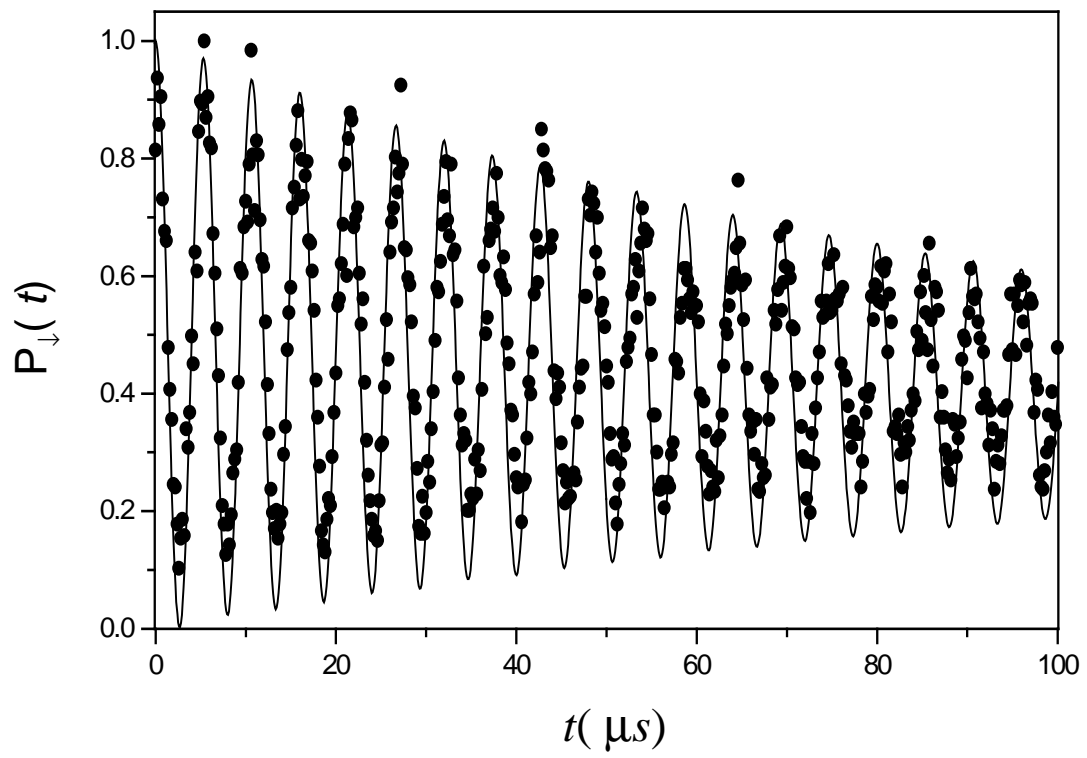


FIG.3

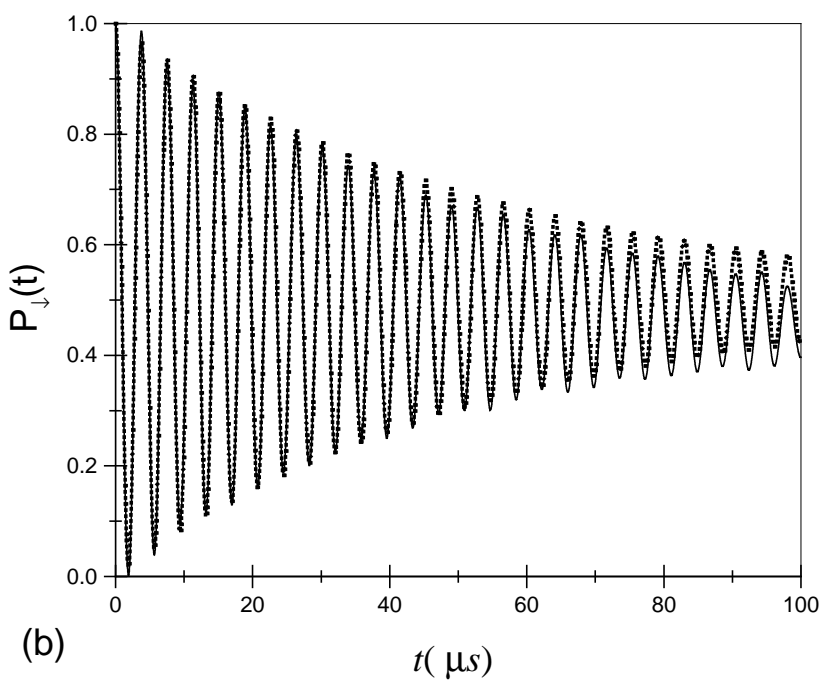
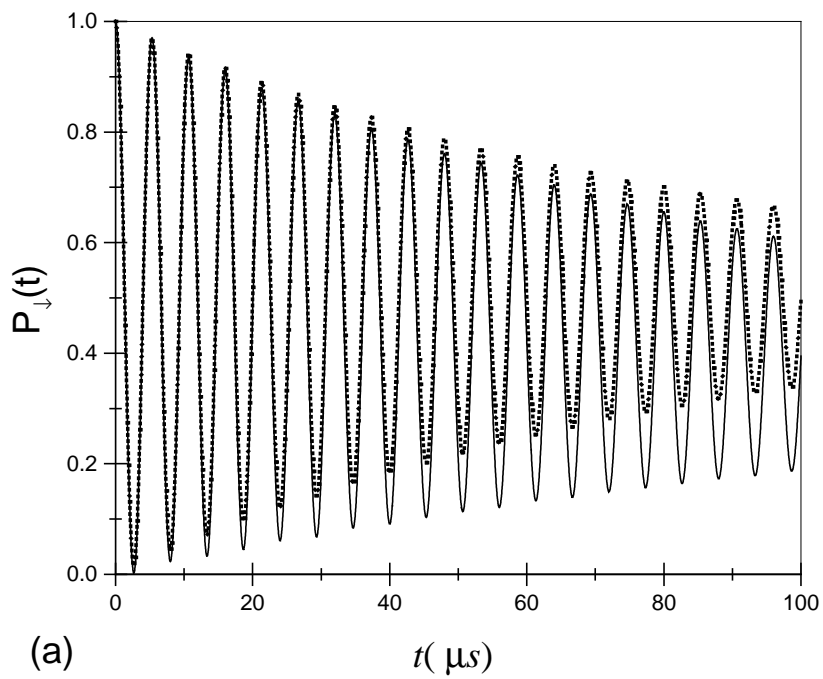


FIG.4.

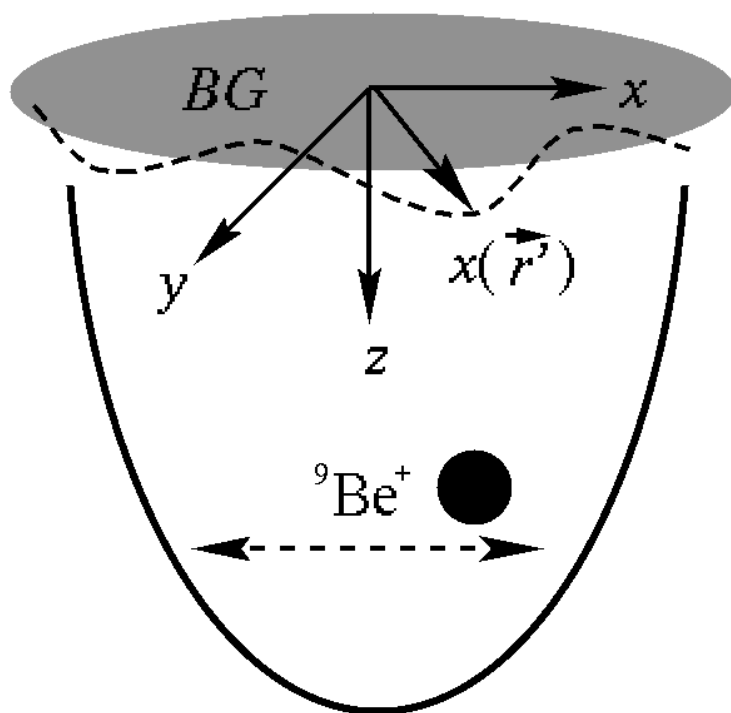


FIG. 5